COMPUTATIONAL AND SPECTROSCOPIC STUDY OF GOLD NANOPARTICLES AND FLUORESCEINAMINE INTERACTIONS

KAREN GUZMÁN [1*], LORENA MENESES [1]
[1*] Escuela de Ciencias Químicas, Pontificia Universidad Católica del Ecuador, Quito, Ecuador

E-mail: kdguzman@puce.edu.ec

Received
Accepted for publication
Published

Abstract

Computational Chemistry is a valuable tool to determine with precision the properties of a system to understand its viability. Thus the interaction energies of fluoresceinamine and gold clusters of 1,3,5,7 gold atoms were calculated by the DFT method B3LYP and 6-311G** and LANL2DZ basis, with the purpose of evidencing a complex formation between the fluorophore and AuNPs. The calculations demonstrate the most stable complex is formed between the 3AuNPs and the primary amine of fluoresceinamine. This is favorable because amines are present in many biological molecules. The results were corroborated by theoretical and experimental UV-Vis and IR Spectroscopy.The theoretical and experimental spectrum of the formation of the complexes was corroborated between the AuNPs and the fluorophore.

Keywords: fluoresceinamine, gold, cluster, interaction, energy.

1. Introduction

Nanoparticles are particles with a size between 1 to 100 nm. They can be classified according to their properties, morphology, and size (Khan, Saeed and Khan, 2019). Metal nanoparticles (MeNPs) present excellent applications in science and technology due to their unique optic properties which depend on their size. MeNPs can emit different colors depending on the absorption bands in the visible region. Also, MeNPs have a high specific surface area that is governed by their size, shape, temperature, and crystalline structure (Molleman and Hiemstra, 2018). Hence, MeNPs are suitable for tissue three-dimensional imaging, and real-time monitoring of surface processes and biosensors (Hammami *et al.*, 2021).

In particular, gold nanoparticles, AuNPs, with diverse sizes and shapes exhibit optoelectronic properties, large surface-volume ratio, low toxicity, and biocompatibility (Yeh, Creran and Rotello, 2012), making them highly useful for medical diagnosis of diseases such as cancer. As a result, these nanoparticles have been investigated as prospective therapeutic agents to detect and cure cancer, drug administration, photothermal and contrast agents, and radiosensitizers (Singh *et al.*, 2018). An example of the application of AuNPs in diagnostic methods is the result of surface plasmon resonance (SPR) with real-time monitoring. Nonetheless, new methods are necessary to develop because of the lack of instrumentation and specificity of the technique (Liu *et al.*, 2021).

Fluorescence is a phenomenon produced when molecules known as fluorophores absorb electromagnetic energy. The absorption of this energy excites the molecules temporarily to a higher energetic state. As a result, to return to its original energetic state, the fluorophore emits light/energy with a different wavelength than the incident wave. This happens whenever

an active source allows a continuous excitation; otherwise, the fluorescence emission stops almost immediately (Bennet, 2020). Hence, fluoresceinamine and other fluorophores like fluorescein and rhodamine have demonstrated high applicability in medical and biological sciences for their ability to be used as biologic markers (Zheng *et al.*, 2013). Fluoresceinamine (FL), Figure 1, is a molecule derived from fluorescein. It is part of the aromatic organic group named xanthenes, whose structures contain two benzene rings attached to a pyran. The other part of the structure is the benzofuranone, composed of a furanone attached to a benzene ring, which has a primary amine bonded to the fifth carbon. These structural differences in xanthenes have allowed the design of biomarkers with photophysical properties such as high photostability and long wavelengths of fluorescence emission (Zheng *et al.*, 2013).

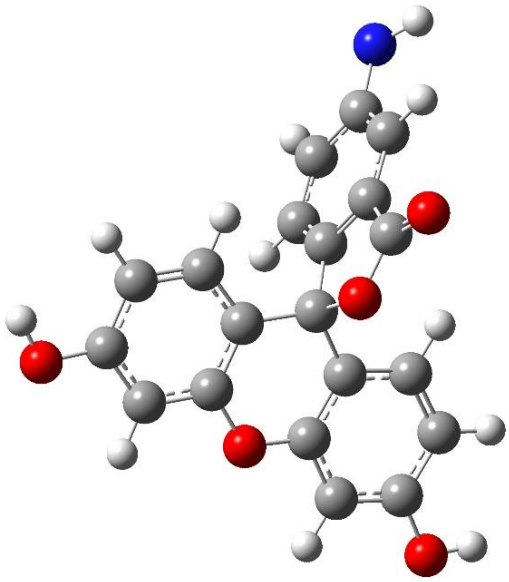

Figure 1. Fluoresceinamine designed in GaussView 5.0

Consequently, computational studies about fluorophores interactions with silver nanoparticles, AgNPs systems have been pursued. Previous studies suggested a high dependency between fluorophore orientation, nanoparticle size, metal-fluorophore distance, and MeNPs dimers (Chowdhury *et al.*, 2009). In addition, fluorescence emissions from the fluorophore and AgNPs system demonstrated intensity and angular variations according to dipole orientations, AgNPs size, and metal-dipole separation (Chowdhury *et al.*, 2007).

In the study of Chowdhury *et.al.* (2007), to understand the behavior of fluoresceinamine-AgNPs, the nanoparticles were placed at the origin of the plane with a distance in the X-axis of the Alexa Fluor fluorophore which was the parameter to range. Computationally, finite difference time domain (FDTD) methods have been used to understand the effects of emission which can be applied to molecular spectroscopy and fluorescence detection. Also, density functional theory (DFT) was used to elucidate the chemical and physical properties of nonbonding interactions between organic molecules such as carbohydrates and AgNPs identifying the diverse interaction of the optimized geometries (Gallegos *et al.*, 2022).

In addition, Pal *et al.* (2018) demonstrated that the interactions between fluorescein and AuNPs with spherical morphology form dimers whose computational spectral results of Visible Ultraviolet Spectroscopy (UV-Vis) and Fourier transform infrared Spectroscopy (FT-IR) show hydrogen bond interactions among two fluorophore molecules when the spherical nanoparticles are being absorbed and the fluorescence time of the system.

Similarly, experimental studies of iron nanoparticles, FeNPs, and fluorescein demonstrated that the fluorophore intensity increases nine times in the far-field and 190 to 450 times in the near field because of the FeNPs, which enhances fluorescence emission (Zhang *et al.*, 2010). In consequence, other studies with other, MeNPs like AuNPs and fluorophores such as fluoresceinamine suggest that this system can be to be viable to demonstrate the capacity of the fluorophore as a biological

marker. As a result, in this work, interaction energies between fluoresceinamine and AuNPs will be determined by Computational Chemistry calculations in order to demonstrate the applicability of the FL-AuNPs complex as a biological marker. The study will be complemented with simulations of UV-Vis and IR spectroscopy to contrast their variations with experimental spectroscopic results.

2. Experimental methods

2.1. Computational Methodology

2.1.1. Geometry Optimization

GaussView 5.0 was used to draw the structures of fluoresceinamine (FL) and the gold nanoparticles (AuNPs) (Gallegos *et al.*, 2022 ; Hratchian *et al.*, 2009). Different planar and non-planar conformations of three, five, and seven gold atom clusters were designed.

The drawn geometries were optimized with Gaussian09 package of programs (Gallegos *et al.*, 2022; Frisch *et al.*, 2009) by using Density Functional Theory (DFT). The chosen method was the B3LYP method. A 6-311G** basis was chosen for fluoresceinamine since it allows quantitative and qualitative results for organic molecules. Whereas for the AuNPs, LANL2DZ basis was used due to its applicability for transition metals like gold (Tomberg, 2013).

2.1.2. Energy interactions calculations

After the geometry optimization, one gold atom was placed at a distance of 7Å between the FL electronegative atoms (e.g., oxygen and nitrogen). The energy interaction calculations were performed using the LANL2DZ bases. The remaining clusters, that were optimized, were located at 7Å between the primary amine of fluoresceinamine and the optimized geometries of the AuNPs.

2.1.3. Spectroscopic Studies

Computational Fourier Transform Infrared Spectroscopy (FTIR) did not require an additional calculous, because its results are obtained from geometry optimization and energy interactions calculous with the Keyword FREQ. For computational Ultraviolet-Visible (UV- VIS) Spectroscopy, the B3LYP method, and LANL2DZ bases were employed with the keyword DT which allows a calculus in an excitement state using DFT.

2.2. Experimental Methodology

2.2.1. Spectroscopic Studies.

To characterize the synthesized fluoresceinamine and AuNPs coated with fluoresceinamine provided by the Laboratory of PUCE Nanomaterials, IR, and UV-Vis studies were done. For the IR spectroscopic study, 3 mg of the fluorophore was located at the sample holder of the IR spectrometer PERKIM ELMER SPECTRUM BX FT-IR. The sample did not require a previous treatment because the instrument has total attenuated reflectance (ATR), allowing the analysis of liquid and solids state molecules. The range of work frequency was from 520 cm^{-1} to 4000 cm^{-1}.

The UV-Vis study required a solution of 16 mg of FL dissolved in 7 mL of acetone with 13 mL of water, 3 drops of the solution were collocated in a quartz cell with water. The working range was between 300 to 700 nm with the equipment AGILENT CARY 60 (Laina, 2010). The same procedure was done with the liquid AuNPs coated with FL.

3. Results and discussion

3.1. Optimized geometries and interaction energies

The geometries of fluoresceinamine (Figure 1) and gold nanoparticles of one, three, five, and seven atoms were optimized For instance, different geometries of nanoparticles were designed, whose best results are summarized in Figure 2. Three gold atom cluster presents a 140.9° angle and equal bonds of 2.6 Å, five gold atom cluster presents angles of 118.5° and 118.4° with

bonds of 2.8 Å and 2.7 Å and seven gold atom cluster has angles of 63.7°, 68.6°C, 63.5°and 60.4°C with bonds of 2.7 Å and 2.8 Å.

During the present investigation, the mentioned results of all the different designed geometries of nanoparticles kept planar geometries just as was proved by Gallegos *et al* (2022), their research bear out that planar geometries are more stable than non-planar geometries. In the particular case of clusters of five and seven gold atoms, non-planar geometries were possibly designed but with DFT calculations planar geometries were once again obtained. Then, to determine the interaction energies between fluoresceinamine and gold clusters, the optimized geometries of the fluorophore and gold atom clusters were located at a distance of 7Å from the primary amine of FL, this value decreased after computational calculations, as shown in Figure 3. Where the smallest interatomic distance was between FL with 5Au atom cluster (2.3 Å), then 1Au atom (2.5 Å), 7Au atoms (4.5 Å), and 3Au atoms (4.9 Å).

Those results are complemented by the interaction energy values because the lowest ones are from cluster of 3Au atoms that presented the lowest energy value of 283.1 kcal, followed by 285.5 kcal from 7Au atoms, while higher values are 288.1 kcal for 5Au atoms and 294.3 kcal for 1Au atom . The results of interaction energies are summarized in Table 1 and were calculated using equation 1.

$$\Delta E_{int} = \Delta E_{Reagents} - \Delta E_{Complex} \qquad \text{Eq.1}$$

First, AuNPs position with respect to the primary amine of fluoresceinamine was changed because, with this functional group, the initial interaction energies tests had lower values, rather than other electron-donating groups such as hydroxyls groups of the xanthene structure as well as the carbonyl of benzofuranone. This is corroborated by Lyu *et al.* (2023) in the analysis of the amines effect in organic molecules with planar gold nanoparticles, hence the Au-N interaction is weak because it does not change the crystal structure even if AuNPs were very small. In addition, the interaction is relevant because this amino group is present in biological molecules such as proteins thus the amine interaction with AuNPs can be used to generate specific applications in biomedicine (González, Acuña and Quiroz, 2022; Lyu *et al.*, 2023;)

After obtaining the interaction energies results of the amine with AuNPs clusters, the complex between the amine group of fluoresceinamine with the 3Au cluster demonstrated the lowest interaction energy (283.1 kcal) with the longer distance (4.9 Å) between the primary amine and AuNPs. This has also been confirmed in Lyu *et al.* (2023) computational analysis, because AuNPs interact favorably with the nitrogen-free pair electrons, with favorable binding and stabalilized complexes, where AuNPs are the metallic center. The interaction energies values of 7Au atoms (285.5 kcal) and 5Au atoms (288.1 kcal) demonstrate that as Au clusters are composed of more atoms, the Au clusters have more interaction with different fluorophore areas. The opposite situation happens with 1Au atom with FL, because this complex has the highest interaction energy (294.3 kcal) (Gallegos *et al.*, 2022). Therefore, with the exposure before is inferred that the N-Au interaction is related to the position, morphology, and size of Au atoms.

During the computation of the Density Functional Theory (DFT) the method B3LYP was employed, which objective is to obtain the system total energy and the distribution of electronic density in its fundamental state without using the system wave function (Piela, 2007). This method was implemented because the results considerate metals such as Au. The basis 6-311G** and LANL2DZ have advantages above other basis whose results are easily obtained with accuracy and without a high computational cost (Rychkov, 2020). This was evident during the results even if the Gaussian computation was extense the energy interaction values were consistent with each other.

To demonstrate that no bond was formed between fluoresceinamine with any gold cluster, their HOMO molecular orbitals were visualized, (Figure 4). In the case of 3Au and 7Au clusters is graphically evident that the electronic density is focused on AuNPs rather than in the fluorophore. This could explained as the HOMO is the highest occupied molecular orbital where the pair of electrons can be easily transferred (Hatsudy, 2020), and graphically the HOMOS of gold and amino have free electrons indication no bond formation. Also, in the particular case of 5Au atoms cluster, the electronic density predominates in the fluorophore, this can be explained because LANL2DZ basis has limitations and it is suggested to use another base that allows a more accurate calculation for this cluster. This was not applied in the present investigation due to the hardware and software limitations of the computers used in this study.

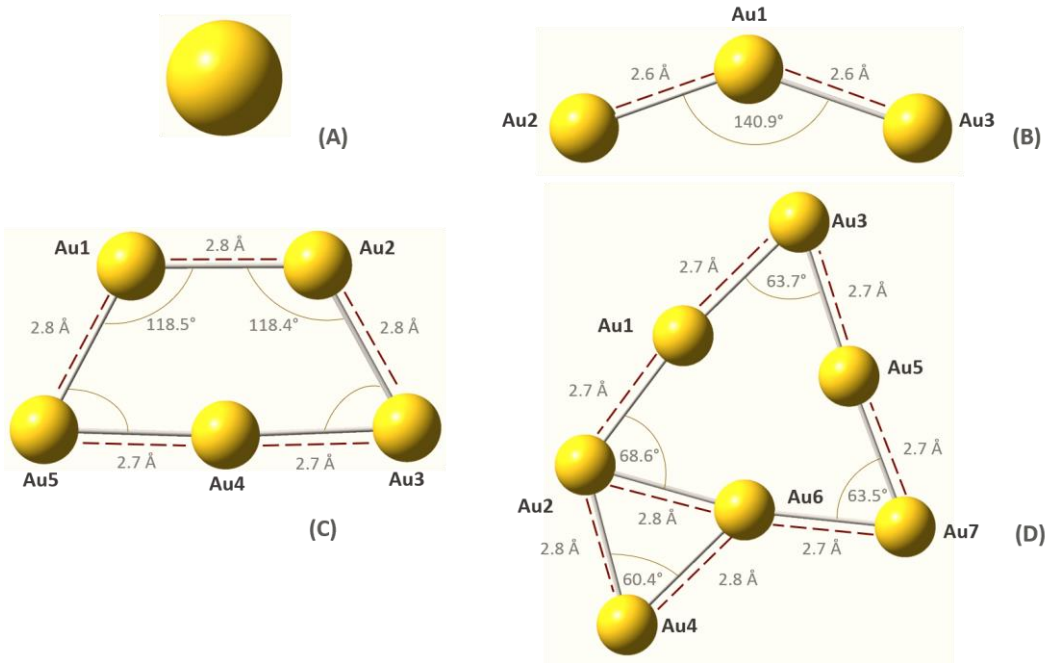

Figure 2. Stable geometries of (A) 1, (B) 3, (C) 5, and (D) 7 gold nanoparticles, obtained by Gaussian09

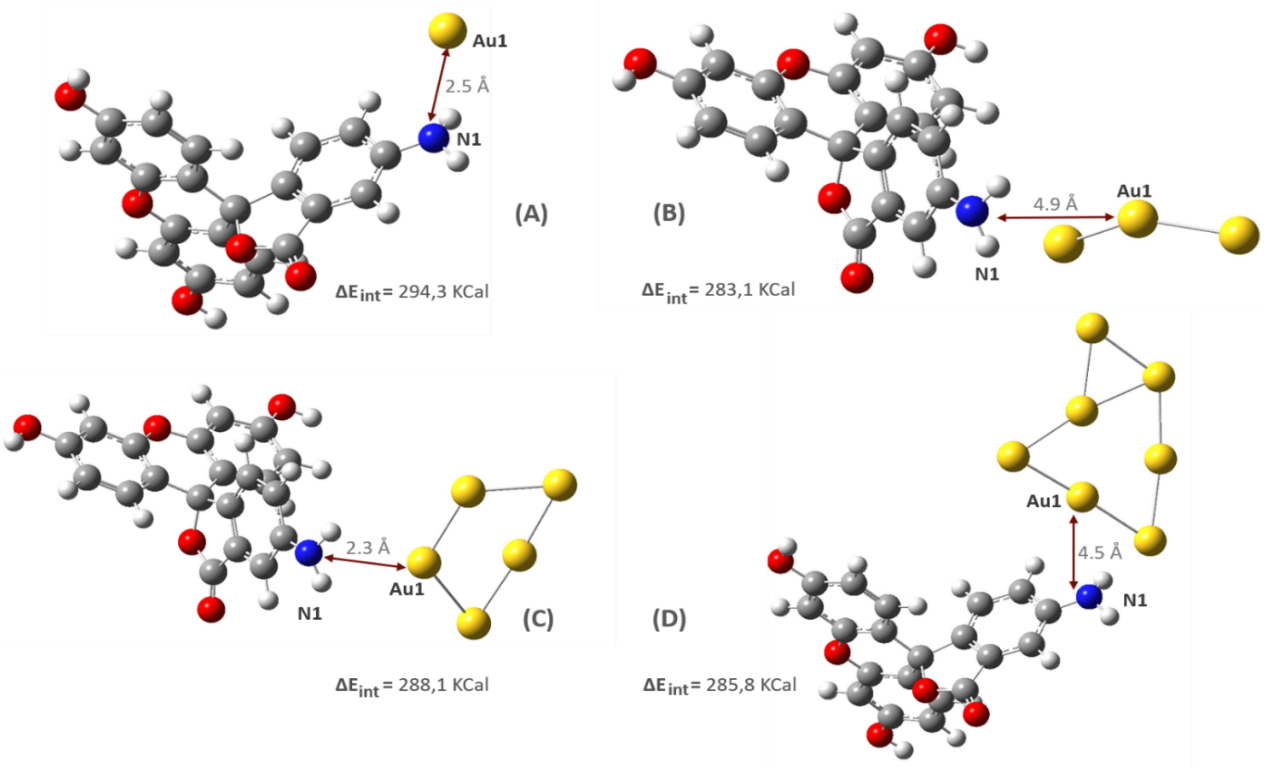

Figure 3. Stable geometries and interaction energies of (A) 1, (B) 2, (C) 5, and (D) 7 gold nanoparticles with fluoresceinamine obtained by Gaussian09

Table 1. Interactions energies of 1, 2, 5 and 7 gold nanoparticles with fluoresceinamine.

Interaction	Distance (Å)	ΔE_{int} (kcal)
1Au_fluorescenamine	2.5	294.3
3Au_fluorescenamine	4.9	283.1
5Au_fluorescenamine	2.3	288.1
7Au_fluorescenamine	4.5	285.8

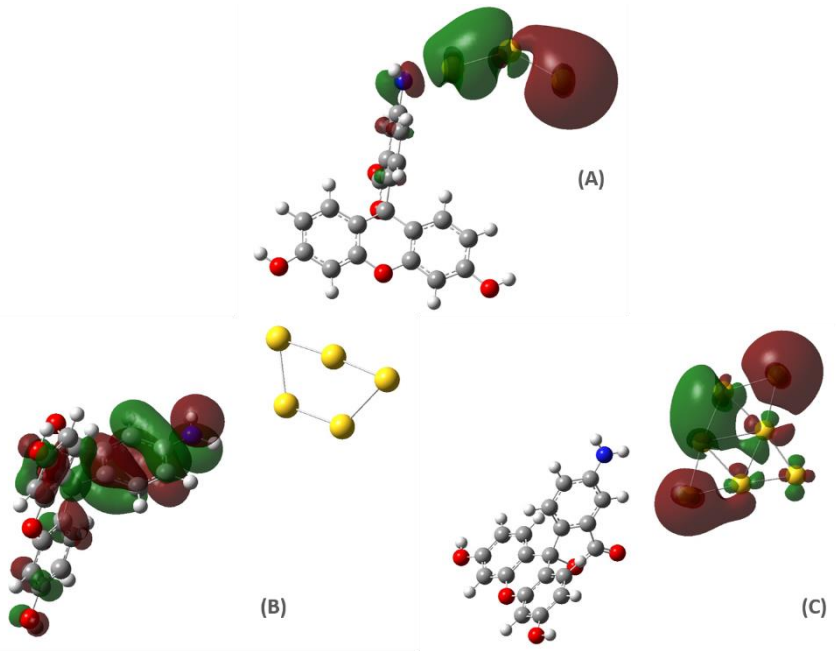

Figure 4. Molecular HOMO orbitals of the interaction of (A) 3, (B) 5, and (C) 7 gold nanoparticles with fluoresceinamine, obtained by Gaussian09 calculations

3.2. UV-Vis Spectroscopy

The results of the theoretical and experimental UV-Vis spectrums are quite similar. The theoretical spectra results (Figure 5a and b) were obtained with Gaussian 09 and the others (Figure 6) are experimental spectrums of AuNPs coated with fluoresceinamine (red line) and only fluoresceinamine (yellow line), all these results are summarized in Table 2. The relation between theoretical and experimental UV-Vis spectrum is noticeable because all the signals have the same shape. Indeed the variations of wavelenght can be explained.

Figure 6 shows a maximum absorption wavelength of 490 nm for synthesized gold nanoparticles coated with fluoresceinamine, which was provided by PUCE Nanomaterials Laboratory. This value is consistent with the literature because spherical AuNPs exhibits an absorption band between 500 and 600 nm, the range is explained because as the size of the NPs increases, the absorbance wavelength value increase as reason to the redshift, due to the fact that the electrons oscillate more in a larger area (Edinburg Instruments, 2023). Therefore, the maximun absortion wavelenght of AuNPs complex with fluoresceinamine (490 nm) is lower from what is reported in the literature and it is explained because coated AuNPs seems to have a smaller particle size, due to factors such as the volumen of the reducing agent, that in higher quantities produces smaller

nanoparticles (De Lamo Santamaría, 2015). Also in other investigations is evident that in UV-Vis spectra of AuNPs coated with organic molecules their absorption wavelenght shifts to higher or smaller wavelenghts (González, Acuña and Quiroz, 2022).

The absortion wavelenght of sinthezized fluoresceinamine (Figure 6, yellow line) is 450 nm while in literature the maximun absortion is above 450 to 495 nm (Bai *et al.*, 2015). This change in wavenumber is explained by the solvent effect of the polar solvent acetone, in this case during ground state, acetone may form a stronger hydrogen bond than in excited state causing an increse of transition energy and a shorter wavelenght (Pavia *et al.*, 2013). In contrast of the experimental spectra, the absorption wavelength of gold nanoparticles in the theoretical UV-Vis spectra (Figure 5, b) is 700 nm and for fluoresceinamine (Figure 5, a) is 265nm.

The changes in theoretical and experimental wavenumber values are different from the literature because DFT integration grids lack rotational invariance producing uncertainties in energy results due to the molecular orientation of the system (Bootsma and Wheeler, 2019). This has also been confirmed in the study of Lemonick (2019) about free energy results that varied in 5 Kcal which generates changes in the regioselectivity and stereoselectivity of the reaction. Because of that, other computational methods can be applied such as TD-DFT, which works with a Polarisable Continuum Model that estimates the effects of the medium of the molecule, solvent, considerating the interactions of hydrogen bonds, π interactions, ion pairing and more without a high computational cost (Adamo and Jacquemin, 2013).

Theoretical UV-Vis Spectra

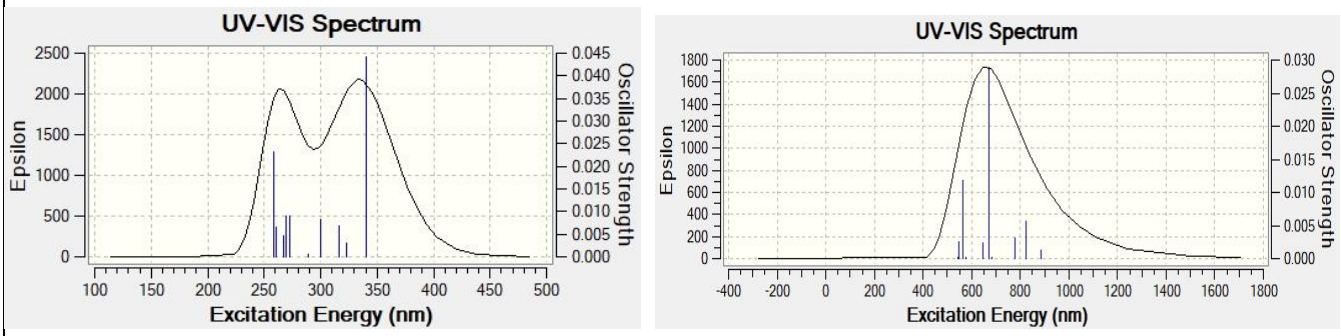

a. *b.*

Figure 5. (a) Theorical UV-VIS Spectrum of fluoresceinamine, (b) theorical UV-VIS Spectrum of of fluoresceinamine and AuNPs complex.

Experimental UV-Vis Spectra

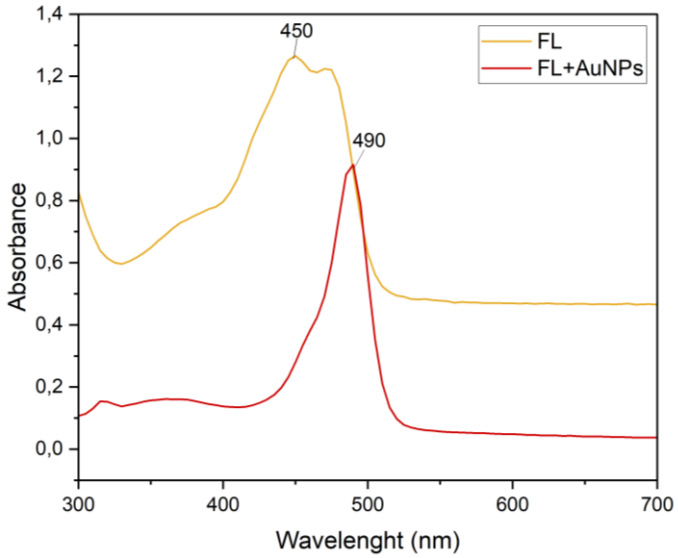

Figure 6. Experimental UV-VIS Spectrum of fluoresceinamine (yellow) and fluoresceinamine-AuNPs complex (red)

Table 2. Maximun absortion wavelenghts of fluoresceinamine and AuNPs complex with fluoresceinamine.

System	Theoretical Wavelenght (nm)	Experimental Wavelenght (nm)	Reference Wavelenght (nm)
Synthesized FL	295	450	450-495
Complex of FL-AuNPS	700	490	500-600

3.3. Infrared Computational and Experimental Spectroscopy

Infrared spectroscopy is a useful tool because their results act like a molecule fingerprint, related with the vibrational frequency and bands position that depends on nature bond (Field, Sternhell and Kalman, 2013), consecuently is an important analytic technique. Therefore in the present investigation, simulated FTIR was study. Most of the results of spectra agree with the values from the literature (SDBS, 2022), summarized in Table 3, although smaller differences in the wavenumber displacement because fluorescenamine is in solid state during the experimental analysis and in gas state in the computational study. These varitions are seen in the O-H and N-H bonds of all the spectra.

Particularly in the FL-AuNPs complex, N-H bond signals (3500-3100 cm^{-1}) of fluoresceinamine are important and their shapes are well defined in theoretical and experimental spectrum of only fluoresceinamine (Figures 7a and 8a), which are not seen in the experimental spectrum of FL-AuNPs complex (Figure 8b) because in N-H range the signal is overlaped. This behavior does not happen in the theoretical spectrum of FL-AuNPs complex (Figure 7b) as a result of N-H signal (3596-3494 cm^{-1}) that according to the literature it will be expected AuNPs are going to be capping by the fluorophore through the primary amine, just as the interaction of other bonds as O-H and C=O (Jayaseelan *et al.*, 2013). Despite that, with the FTIR spectra of fluoresceinamine the fluorophore has been characterized. The O-H stretching (3444 cm^{-1}) shifts to 3832 cm^{-1}, N-H bands of the primary amine (3342 and 3220 cm^{-1}) shifts to 3671 and 3572 cm^{-1}, the C=O of the lactone (1588 cm^{-1}) shifts to 1838 cm^{-1}, C-O of xanthene (1379 cm^{-1}) changes to 1300 cm^{-1}, C-O of lactone (1319 cm^{-1}) decreases to 1209 cm^{-1} and C=C of the aromatic rings (1469 cm^{-1}) shifts higher to 1471 cm^{-1} (Pavia *et al.*, 2013) , in brief the computational results are favorable and summarized in Table 3.

Theoretical IR Spectra

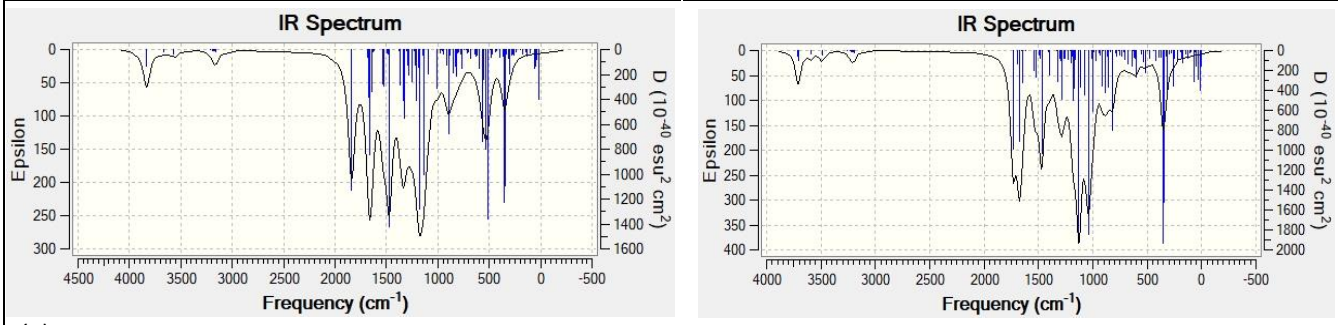

(a) *(b)*

Figure 7 . (a) Theoretical FTIR Spectrum of fluoresceinamine, (b) Theoretical FTIR Spectrum of fluoresceinamine and AuNPs complex.

Experimental IR Spectra

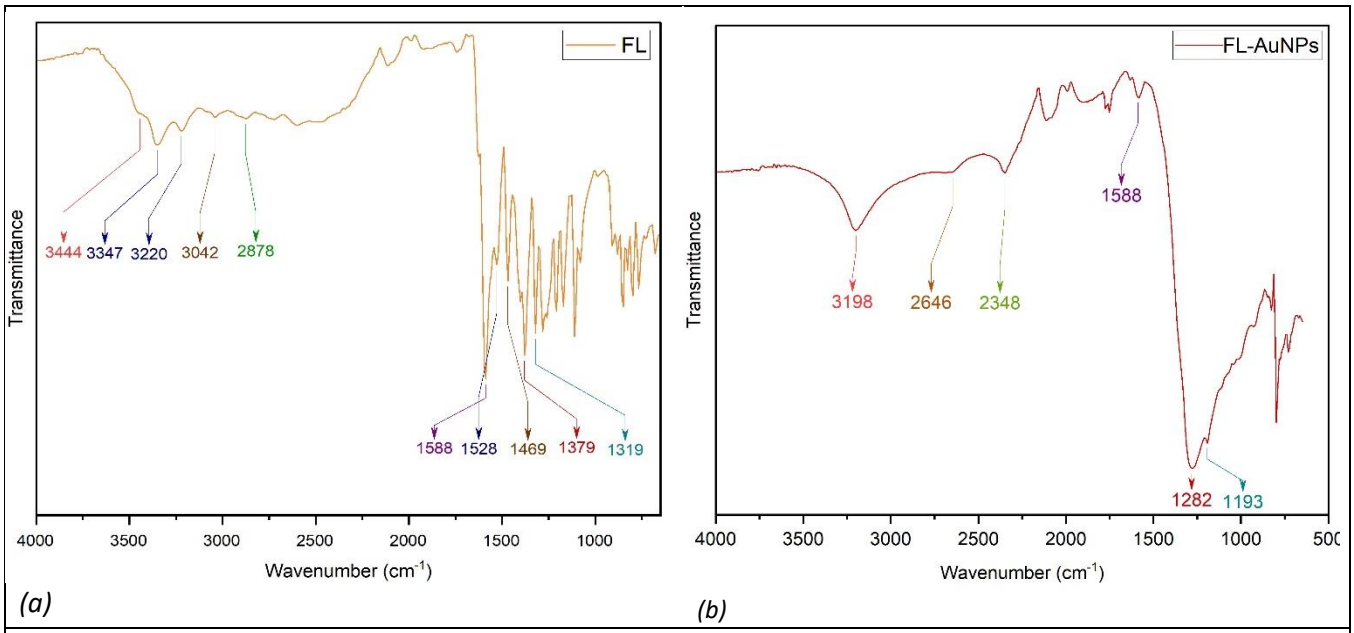

Figure 8 . *(a)* Experimental FTIR Spectrum of fluoresceinamine and *(b)* experimental FTIR Spectrum of fluoresceinamine and AuNPs complex

Table 3. Experimental and theoretical FTIR frequencies of fluoresceinamine and fluoresceinamine - AuNPs complex.

FTIR Spectra Results							
Functional Group	Bond	Range (literature)	Fluoresceinamine		Fluoresceinamine and AuNPs Complex		Vibration
			Experimental Frequency (cm^{-1})	Theoretical Frequency (cm^{-1})	Experimental Frequency (cm^{-1})	Theoretical Frequency (cm^{-1})	
Alcohols	O-H	3400-3200	3444	3832 (asy) 3833 (sym)	3198	3710 (asy)	s
Primary Amine	N-H	3500-3100	3342 3220	3671 (asy) 3572 (sy)	-	3596 (asy) 3494 (sy)	s
	N-H	1640-1550	1528	1657	-	1696	b
	C-N	1350-1000	1103	1093	1193	1192	b-r
Alkanes	C-H (sp2)	3040-3125	3042	3157	2646	3203	s

	(sp3)	2800-3000	2878	3211	2348	3195	s
	C=C	1600-1475	1469	1471	1469	1642	s
Ester	C=O	1750-1730, FL spectra 1600*	1588	1838	1588 (minor transmittance)	1733	s
Ester	C-O	1300-1000	1319	1209	1193	1157	s
Ether			1379	1300	1282	1302	

Conclusions

Interaction energies between fluoresceinamine and AuNPs were determined using computational methods. The lower interaction energy (283.1 kcal) evidenced the most stable complex with the primary amine of the fluorophore and 3AuNPs, this was possible by the optimized geometries of fluoresceinamine, 1AuNPs, 3AuNPs, 5AuNPs, and 7AuNPs clusters using the DFT method B3LYP and 6-311G** and LANL2DZ basis set. Also, the research was complemented with theoretical and experimental UV-Vis Spectroscopy and IR Spectroscopy. The theoretical absorbance results of UV-Vis spectrum are not the same as the values from the literature. On the other hand, the theoretical IR spectroscopy agrees with the literature values. Nonetheless, the shift results in the UV-Vis spectra demonstrating the interactions between the fluorophore and the AuNPs, also the decreased signal in the IR theoretical and experimental spectra corroborate the complex conformation.

Acknowledgements

I appreciate Lorena, my thesis tutor, who supported me during this research process, sharing her appreciated time, guide, and experience in Computational Chemistry. I also thank María Fernanda, who taught me the amazing world of nanotechnology. To Pamela for her guidance and motivation during the redaction process. Also, to my dear professor Amanda who has led me to think like a chemist. And thank you to everyone who has helped me to carry out this project since day one.

References

Adamo, C. and Jacquemin, D. (2013) 'The calculations of excited-state properties with time-dependent density functional theory', *Chemical Society Reviews*, 42(3), pp. 845–856. doi: 10.1039/c2cs35394f.

Bai, Z. *et al.* (2015) 'Fluorescence resonance energy transfer between bovine serum albumin and fluoresceinamine', *Luminescence*, 31, p. 69. doi: 10.1002/bio.3012.

Bennet, T. (2020) *Fluorescein Fundamentals*. Available at: https://www.opsweb.org/page/FA.

Bootsma, A. N. and Wheeler, S. E. (2019) 'Popular integration grids can result in large errors in DFT-computed free energies', *ChemRxiv*, pp. 1–20.

Chowdhury, M. *et al.* (2009) 'Computational study of the interaction of fluorophores with various metallic nanoparticle systems', *Proc SPIE*. doi: 10.1117/12.809181.

Chowdhury, M. H. *et al.* (2007) 'Computational study of fluorescence scattering by silver nanoparticles', *Journal of the Optical Society of America B*, 24(9), pp. 2259–2267. doi: 10.1364/JOSAB.24.002259.

Field, L. D., Sternhell, S. and Kalman, J. R. (2013) *Organic Structures from Spectra i Fifth Edition*. Fifth Edit. West Sussex: John Wiley & Sons, Ltd.

Frisch, M. . *et al.* (2009) 'Gaussian 09'. Available at: https://gaussian.com/glossary/g09/ (Accessed: 25 March 2023).

Gallegos, F. E. *et al.* (2022) 'Computational Modeling of the Interaction of Silver Clusters with Carbohydrates', *ACS Omega*, 7(6), pp. 4750–4756. doi: 10.1021/acsomega.1c04149.

González, E. E., Acuña, Y. A. and Quiroz, A. M. (2022) 'Nanopartículas de oro funcionalizadas con l-cisteína para detección de arsénico en agua', *Ingeniería Investigación y Desarrollo*, 21(2 SE-Artículos de investigación), pp. 66–72. doi: 10.19053/1900771X.v21.n2.2021.14271.

Hammami, I. *et al.* (2021) 'Gold nanoparticles: Synthesis properties and applications', *Journal of King Saud University - Science*, 33(7), p. 101560. doi: https://doi.org/10.1016/j.jksus.2021.101560.

Hatsudy (2020) *HOMO and LUMO: Energy of Bonding Orbital and Antibonding Orbital ｜ Hatsudy*. Available at: https://hatsudy.com/homo.html (Accessed: 9 June 2023).

Hratchian, H. P. *et al.* (2009) 'GaussView 5'.

Jayaseelan, C. *et al.* (2013) 'Green synthesis of gold nanoparticles using seed aqueous extract of Abelmoschus esculentus and its antifungal activity', *Industrial Crops and Products*, 45, pp. 423–429. doi: https://doi.org/10.1016/j.indcrop.2012.12.019.

Khan, Ibrahim, Saeed, K. and Khan, Idrees (2019) 'Nanoparticles: Properties, applications and toxicities', *Arabian Journal of Chemistry*, 12(7), pp. 908–931. doi: https://doi.org/10.1016/j.arabjc.2017.05.011.

Laina, J. (2010) *Degradación de la Fluoresceína sódica por fotoatálisis heterogénea en un reactor heliofotocatalítico.* Universidad Tecnológica de Pereira.

De Lamo Santamaría, B. (2015) *Obtención y caracterización de nanopartículas de oro a partir de mostos*. Universidad de Valladolid.

Lemonick, S. (2019) *Density functional theory error discovered*. Available at: https://cen.acs.org/physical-chemistry/computational-chemistry/Density-functional-theory-error-discovered/97/web/2019/07 (Accessed: 12 June 2023).

Liu, X.-Y. *et al.* (2021) 'Gold nanoparticles: synthesis, physiochemical properties and therapeutic applications in cancer', *Drug Discovery Today*, 26(5), pp. 1284–1292. doi: https://doi.org/10.1016/j.drudis.2021.01.030.

Lyu, Y. *et al.* (2023) 'The Interaction of Amines with Gold Nanoparticles.', *Advanced materials (Deerfield Beach, Fla.)*, p. 1. doi: 10.1002/adma.202211624.

Molleman, B. and Hiemstra, T. (2018) 'Size and shape dependency of the surface energy of metallic nanoparticles: unifying the atomic and thermodynamic approaches', *Physical Chemistry Chemical Physics*, 20(31), pp. 20575–20587. doi: 10.1039/C8CP02346H.

Pal, G. D. *et al.* (2018) 'Interactions of Fluorescein Dye with Spherical and Star Shaped Gold Nanoparticles.', *Journal of nanoscience and nanotechnology*, 18(4), pp. 2943–2950. doi: 10.1166/jnn.2018.14350.

Pavia, D. L. *et al.* (2013) *Introduction to Spectroscopy*. Fifth Edit. Washington: Cengaage Learning.

Piela, L. (2007) 'Electronic motion: Density Functional Theory (DFT)', in *Ideas of Quantum Chemistry*. Amsterdam: Elsevier, pp. 567–614. doi: https://doi.org/10.1016/B978-044452227-6/50012-0.

Rychkov, D. (2020) 'A Short Review of Current Computational Concepts for High-Pressure Phase Transition Studies in Molecular Crystals', *Crystals*, 10, p. 81. doi: 10.3390/cryst10020081.

SDBS, S. D. for O. C. (2022) *IR: KBr disc - 5 Aminofluorescein*. Available at: https://sdbs.db.aist.go.jp/sdbs/cgi-bin/direct_frame_top.cgi (Accessed: 7 June 2023).

Singh, P. *et al.* (2018) 'Gold Nanoparticles in Diagnostics and Therapeutics for Human Cancer', *International Journal of Molecular Sciences*. doi: 10.3390/ijms19071979.

Tomberg, A. (2013) *An Introducction to Computational Chemistry Using G09W and Avogadro doftware.* Available at: https://barrettgroup.mcgill.ca/tutorials/Gaussian tutorial.pdf.

Yeh, Y.-C., Creran, B. and Rotello, V. M. (2012) 'Gold nanoparticles: preparation, properties, and applications in bionanotechnology.', *Nanoscale*, 4(6), pp. 1871–1880. doi: 10.1039/c1nr11188d.

Zhang, Y. *et al.* (2010) 'Interactions of Fluorophores with Iron Nanoparticles: Metal-Enhanced Fluorescence', *The Journal of Physical Chemistry C*, 114(17), pp. 7575–7581. doi: 10.1021/jp910080b.

Zheng, H. *et al.* (2013) 'Advances in modifying fluorescein and rhodamine fluorophores as fluorescent chemosensors', *Chemical Communications*, 49(5), pp. 429–447. doi: 10.1039/C2CC35997A.